Development of prestressed unbonded and bonded CFRP strengthening solutions for tensile metallic members

Ardalan Hosseini [1,2*], Elyas Ghafoori [1,3], Masoud Motavalli [1,4], Alain Nussbaumer [2], Xiao-Ling Zhao [4], Riadh Al-Mahaidi [3] and Giovanni Terrasi [5]

[1] *Structural Engineering Research Laboratory, Swiss Federal Laboratories for Materials Science and Technology (Empa), Dübendorf, Switzerland*
[2] *Resilient Steel Structures Laboratory, Swiss Federal Institute of Technology Lausanne (EPFL), Lausanne, Switzerland*
[3] *Department of Civil and Construction Engineering, Swinburne University of Technology, Melbourne, Australia*
[4] *Department of Civil Engineering, Monash University, Australia*
[5] *Mechanical Systems Engineering Laboratory, Swiss Federal Laboratories for Materials Science and Technology (Empa), Dübendorf, Switzerland*

Abstract

In this study, a novel unbonded mechanical clamping system was developed for the strengthening of tensile metallic members using prestressed carbon fiber reinforced polymer (CFRP) plates. The system clamps a pair of prestressed CFRP reinforcement to a metallic substrate and provides an almost uniform contact pressure over the CFRP plate along the anchorage length. A finite element simulation was used to optimize the design of the mechanical components of the system. Subsequently, a set of static and fatigue tests was performed to evaluate the performance of the optimized design. Experimental results revealed that the proposed mechanical clamping system is capable of transferring the entire tensile capacity of the CFRP plates to the steel substrate, even after experiencing 10 million fatigue cycles. The comparative performance of the developed clamps was further investigated by a set of static tests on steel plate specimens strengthened with the prestressed bonded reinforcement (PBR) and the newly developed prestressed unbonded reinforcement (PUR) systems. Furthermore, simple analytical models are proposed to formulate the stress state in prestressed unbonded and bonded CFRP-strengthened tensile metallic members. The accuracy of the proposed analytical formulations was verified by the experimental results obtained during the current study. Experimental results revealed that the efficacy of having relatively high prestressing forces in the normal modulus (NM) CFRP reinforcements is much higher than the stiffness improvement obtained by using ultra-high

* Corresponding author. Structural Engineering Research Laboratory, Swiss Federal Laboratories for Materials Science and Technology (Empa), Überlandstrasse 129, CH-8600 Dübendorf, Switzerland. Tel.: +41 58 765 4766; Fax: +41 58 765 6244. Email addresses: ardalan.hosseini@empa.ch; ardalan.hosseini@epfl.ch.

modulus (UHM) CFRPs. However, the available capacity of the PBR system before debonding failure is far lower than that of the developed PUR solution.

Keywords: Steel structure, fatigue strengthening, carbon fiber reinforced polymer (CFRP), prestressed bonded reinforcement (PBR), prestressed unbonded reinforcement (PUR), ultra-high modulus (UHM) CFRP, analytical solution.

Nomenclature

Latin symbols		**Greek symbols**	
A	Area	α	Thermal expansion coefficient
b	Width	ε	Strain
d	Fillet dimension	λ	Elastic shear stress distribution parameter
E	Elastic modulus	μ	Friction coefficient
$E´$	Dynamic elastic modulus	σ	Normal stress
G	Shear modulus	τ	Shear stress
l	Length	**Subscripts**	
n	Elastic modulus ratio	a	Adhesive
P	Bolt preload/prestress force	f	FRP
R	Fatigue load ratio	g	Glass transition
t	Thickness	pre	Prestressing
T	Tension force or resultants	s	Steel
ΔT	Temperature difference	t	Transformed section
v	Longitudinal displacement	u	Ultimate
		y	Yield

1. Introduction

Today, a large number of existing metallic structures need to be strengthened against fatigue to carry higher service loads and/or be sufficiently safe for a longer service life. The conventional method for the strengthening of ageing metallic structures is to bolt or weld additional steel plates to the tension face of the member, and/or to replace a part of or the entire damaged structural member. It is obvious that these conventional techniques are time-consuming, costly, and not so efficient, as the steel cover plates are usually bulky, heavy, difficult to fix, and prone to fatigue and corrosion [1], while such strengthening methods might not be applicable to all types of existing metallic structures (for instance due to poor weldability of the parent alloy). On the other hand, certain advantages of carbon fiber reinforced polymer (CFRP) composites, such as high corrosion resistance, light weight, high

strength, and fatigue endurance [2], have made CFRP composites a unique alternative for static (e.g., [3-7]) and fatigue (e.g., [8-12]) strengthening of ageing metallic structures.

It is evident that the use of prestressed CFRP composites has several advantages over the nonprestressed reinforcements owing to their ability to reduce the permanent tensile stresses in the strengthened member. Therefore, application of prestressed CFRP reinforcements is of crucial interest for fatigue strengthening of existing metallic structures [13-15], as it can reduce the mean stress levels, and consequently, enhance the fatigue life of the strengthened member [16-18]. Despite this great advantage, fewer attempts have been made to use prestressed bonded reinforcement (PBR) systems for strengthening of steel members in practical cases [19]. This may be explained by the fact that high prestressing levels cannot be reached in PBRs, owing to the premature failure by debonding of the composite reinforcement from the steel substrate [20,21]. Consequently, for the PBR systems to be effective, the high interfacial and peeling stresses generated in the end zones of the prestressed reinforcement should be avoided. Therefore, mechanical end-anchorages are commonly used to deal with the debonding failure of PBRs, although very few laboratory applications of PBR systems without any end-anchorages can be found in the literature [22,23].

In 2015, several laboratory tests were performed at the Structural Engineering Research Laboratory of Empa to compare the behavior of steel beams strengthened by PBR and prestressed unbonded reinforcement (PUR) systems [24]. The results have shown that, when metallic beams are strengthened by prestressed CFRP plates, the static and fatigue performance of the CFRP-strengthened member is more sensitive to the prestressing level than to the existence of the adhesive bond [14,25]. Based on these results, a novel prestressed unbonded CFRP reinforcement system was developed [26] and tested in the laboratory [16]. The system was used for fatigue strengthening of Münchenstein Bridge, a 120-year-old metallic railway bridge in Switzerland [17]. Different possible configurations of the PUR

systems for strengthening of metallic I-beams are suggested in [27]. More recently a flat PUR (FPUR) system was developed by the authors to strengthen real-scale metallic I-beams using prestressed CFRP plates [28]. The system allows for an easy and straightforward on-site post-tensioning of CFRP reinforcements using a set of hydraulic jacks. The developed FPUR system was then used to strengthen the cross-girders of a 122-year-old metallic roadway bridge in Australia [29]. The development, laboratory testing, and field application of the PUR systems, however, have been so far limited to the strengthening of metallic I-beams. On the other hand, in practical cases, there exist many other metallic member configurations, which require static and/or fatigue strengthening. Consequently, there is a need for the development of proper PUR solutions that can be used to strengthen existing tensile metallic members; the present paper addresses the aforementioned issue.

In this study, analytical solutions are firstly proposed to analyze the stress state in prestressed unbonded and bonded CFRP-strengthened steel plates subjected to external tensile loading. Second, a novel friction-based mechanical clamping system is developed for the strengthening of tensile metallic members with prestressed CFRP plates. A finite element (FE) simulation is used to optimize the design of the required mechanical components of the system, and subsequently, the static and fatigue performance of the system is experimentally evaluated. The practical performance of the proposed system is then investigated in a set of static tests conducted on steel plate specimens strengthened with the PBR and the newly developed PUR systems. Lastly, the capability of the proposed analytical modeling to predict the stress state in the nonprestressed/prestressed bonded/unbonded CFRP-strengthened tensile steel members is evaluated using the experimental test results. It is worth mentioning that, the current paper is an extended version of the authors' paper presented in the Fourth Conference on Smart Monitoring, Assessment and Rehabilitation of Civil Structures (SMAR 2017) [30].

2. Analytical Solution

2.1. Prestressed Unbonded Reinforcement (PUR)

The schematic of a tensile steel member strengthened with mechanically anchored prestressed unbonded CFRP reinforcements is shown in Figure 1a. By assuming that the mechanical clamping system does not exhibit any slippage, and the CFRP and steel behave linearly (a reasonable assumption in the case of high cycle fatigue (HCF) loading), the axial stress in the steel substrate (σ_s) and the CFRP reinforcements (σ_f) due to the effect of the external tensile loading (T), CFRP prestrain level (ε_{pre}), as well as any temperature changes after CFRP strengthening (ΔT), can be expressed by solving the force equilibrium and displacement compatibility equations as follows:

$$\sigma_s = \frac{T - 2E_f A_f \left(\varepsilon_{pre} - (\alpha_f - \alpha_s)\Delta T\right)}{A_t} \tag{1}$$

$$\sigma_f = \frac{n\left[T + E_s A_s \left(\varepsilon_{pre} - (\alpha_f - \alpha_s)\Delta T\right)\right]}{A_t} \tag{2}$$

where A_s and A_f are the cross-sectional areas of steel, and the CFRP reinforcements on one side of the steel plate, respectively; E_s and E_f are the elastic moduli of steel and the CFRP composite, respectively; α_s and α_f are the thermal expansion coefficient of steel and the CFRP composite, respectively. Furthermore, $n = \frac{E_f}{E_s}$, and A_t is the transformed cross-sectional area of the joint and is calculated as follows:

$$A_t = A_s + 2nA_f \tag{3}$$

2.2. Prestressed Bonded Reinforcement (PBR)

It is obvious that an elastic-plastic analysis (such as that proposed by Hart-Smith [31]) is required to determine the debonding load of adhesively bonded CFRP-to-steel joints. However, for many applications, such as the design of composite patch reinforcements within the elastic limits, the determination of thermal residual strains due to the curing of the adhesive at elevated temperatures, and the fatigue strengthening of steel members, a simple one-dimensional linear-elastic model can be sufficiently accurate [15,32,33]. Therefore, as the

main intention of the current study is to compare the efficiency of a prestressed unbonded CFRP reinforcement with that of a prestressed bonded one in fatigue strengthening of steel members, the linear-elastic solution developed by Albat and Romilly [32] is deemed to be accurate enough for the determination of stress in the steel substrate. Consequently, in this section, the aforementioned model has been adopted to take into account the effect of a prestressing force in the CFRP reinforcements on the stress reduction and distribution along the steel substrate in an adhesively bonded CFRP-to-steel joint, subjected to external loading.

Figure 1b depicts the schematic of a tensile steel member strengthened with double-sided prestressed bonded CFRP reinforcements. In this case, the governing equilibrium equations can be derived using the free body diagram of an infinitesimal element of the joint, depicted in Figure 2, in conjunction with the selected coordinate systems as shown in Figure 1b. The two differential equations for the horizontal force equilibrium can be expressed as [32,34,35]

$$\frac{\mathrm{d}T_f(y)}{\mathrm{d}y} - b_f \tau_a(y) = 0 \tag{4}$$

$$\frac{\mathrm{d}T_s(y)}{\mathrm{d}y} + 2b_f \tau_a(y) = 0 \tag{5}$$

where b_f is the total width of the individual CFRP reinforcements on one side of the steel plate (if more than one strip is applied), $\tau_a(y)$ is the interfacial shear stress function, and $T_f(y)$ and $T_s(y)$ are axial forces in the CFRPs and steel substrate, respectively:

$$\begin{aligned} T_f(y) &= \sigma_f(y) A_f \\ T_s(y) &= \sigma_s(y) A_s \end{aligned} \tag{6}$$

Considering the prestrain level in the CFRP reinforcements, as well as the effect of temperature changes, the compatibility equations for the CFRP plate, steel substrate, and the adhesive layer can be expressed as:

$$\varepsilon_f(y) = \frac{\mathrm{d}v_f(y)}{\mathrm{d}y} = \frac{T_f(y)}{E_f A_f} - \varepsilon_{pre} + \alpha_f \Delta T \tag{7}$$

$$\varepsilon_s(y) = \frac{\mathrm{d}v_s(y)}{\mathrm{d}y} = \frac{T_s(y)}{E_s A_s} + \alpha_s \Delta T \tag{8}$$

$$\tau_a(y) = G_a \gamma_a(y) = G_a \arctan\left(\frac{v_f(y) - v_s(y)}{t_a}\right) \approx \frac{G_a}{t_a}(v_f(y) - v_s(y)) \tag{9}$$

where $\varepsilon_f(y)$, $\varepsilon_s(y)$, $v_f(y)$ and $v_s(y)$ are axial strain and deformation of CFRP reinforcements and steel substrate, respectively; G_a and t_a are the adhesive shear modulus and thickness, respectively. Differentiating Eq. (9) and substituting Eqs. (7) and (8) into the resultant equation yields to

$$\frac{\mathrm{d}\tau_a(y)}{\mathrm{d}y} = \frac{G_a}{t_a}\left[\frac{T_f(y)}{E_f A_f} - \frac{T_s(y)}{E_s A_s} - \varepsilon_{pre} + (\alpha_f - \alpha_s)\Delta T\right] \tag{10}$$

By differentiating Eq. (10) and substituting the equilibrium equations (i.e., Eqs. (4) and (5)), into the resultant equation, the second-order ordinary differential equation of the adhesively bonded CFRP-to-steel joint in terms of the interfacial shear stress distribution can be obtained as

$$\frac{\mathrm{d}^2\tau_a(y)}{\mathrm{d}y^2} - \lambda^2 \tau_a(y) = 0 \tag{11}$$

where

$$\lambda^2 = \frac{G_a b_f}{t_a}\left(\frac{1}{E_f A_f} + \frac{2}{E_s A_s}\right) \tag{12}$$

Considering the general solution of the obtained differential equation and evaluating its unknown coefficients by applying the boundary conditions of the stress resultants $T_f(y)$ and $T_s(y)$ (see [32] for further details), the interfacial shear stress, as well as the axial stresses in the adherents can be formulated as follows:

$$\tau_a(y) = \frac{G_a}{\lambda t_a}\left((\alpha_f - \alpha_s)\Delta T - \varepsilon_{pre} - \frac{T}{E_s A_s}\right)\frac{\sinh(\lambda y)}{\cosh(\lambda l)} \tag{13}$$

$$\sigma_f(y) = \frac{G_a}{\lambda^2 t_a t_f}\left((\alpha_f - \alpha_s)\Delta T - \varepsilon_{pre} - \frac{T}{E_s A_s}\right)\left(\frac{\cosh(\lambda y)}{\cosh(\lambda l)} - 1\right) \quad (14)$$

$$\sigma_s(y) = \frac{T}{A_s} - \frac{2b_f G_a}{\lambda^2 t_a A_s}\left((\alpha_f - \alpha_s)\Delta T - \varepsilon_{pre} - \frac{T}{E_s A_s}\right)\left(\frac{\cosh(\lambda y)}{\cosh(\lambda l)} - 1\right) \quad (15)$$

where l is half of the CFRP reinforcement length and $-l \le y \le l$. From Eqs. (13)–(15) one can infer that applying prestressed CFRP plates as adhesively bonded reinforcements on a tensile steel member can reduce the stress level in the strengthened member, while leads to a distribution of interfacial shear stresses at the two extremities of the bonded length even at zero external load (T = 0). Careful study of Eq. (13), however, reveals that the prestrain level (ε_{pre}) and the external load (T) have an identical mathematical sign, which reminds that higher interfacial shear stresses are expected in PBR joints compared to a nonprestressed bonded reinforcement (at a known T); this might eventually lead to a lower ultimate capacity (debonding load) in PBR solutions.

3. Development of Mechanical Clamping System

3.1. Design Basis

A schematic cross-sectional view of the proposed mechanical clamping system is illustrated in Figure 3a. As the figure shows, the main idea of the system is to hold the prestressed CFRP plates on the steel substrate (the steel plate in this case) with the help of friction. Therefore, it is necessary to press the prestressed CFRP plates against the steel substrate using a set of prestressed bolts. As the system functions with friction, 3M™ diamond friction shims (3M Technical Ceramics GmbH, Germany) can be used between the CFRP plates and the steel substrate to increase the friction (see Section 4.3.1). Consequently, owing to insights about the static friction in the CFRP-diamond shim, and diamond shim-steel interfaces, the required prestressing force that should be provided by the prestressed bolts can be calculated for a target value of the axial stress in the CFRP plates (herein the tensile strength of the CFRP composite).

Owing to the bending deformation of the clamp plate upon fastening the prestressed bolts (see Figure 3b), it is clear that another mechanical part, called the *hard plate*, is needed to transfer the lateral compression force from the clamp to the CFRP plate through a more uniform distribution, σ_n, and avoid pinching it. The hard plates are toothed on the contact side with the CFRP and they have a hardness of HRC 58(-60) on the Rockwell scale. It is obvious that the fillet dimension of the hard plate (see Figure 3b) is one of the most important parameters affecting the contact stress distribution. Given the complexity of the system, a finite element (FE) simulation was performed to optimize the dimensions of the different mechanical components.

3.2. Finite Element Simulation

3.2.1. *Model description*

Owing to the symmetry of the system, a finite element (FE) model of one fourth of the proposed mechanical clamping system was assembled in ABAQUS [36]. The FE model consisted of a CFRP plate (50 × 1.4 mm) pressed against the steel substrate via the mechanical clamp (see Figure 4a). All the steel components were modelled as an isotropic linear elastic material with an elastic modulus (E_s) and Poisson's ratio (v_s) of 200 GPa and 0.3, respectively. Although a unidirectional CFRP plate indeed exhibits anisotropy, it was also modelled as an isotropic linear elastic material with an elastic modulus (E_f) and Poisson's ratio (v_f) of 160 GPa, and 0.3, respectively, for the sake of simplicity. Indeed, the main intention of the FE simulation was to optimize the dimensions of the steel components and find out the required number and diameter of the prestressed bolts to provide enough friction force between the CFRP plate and the steel substrate; concerning the design of the clamp plates, the anisotropic behavior of the CFRP plate is deemed to have no significant influence on the FE results.

A hard contact was used between the clamp plate, hard plate, CFRP, and the steel substrate in the normal direction. However, using the penalty formulation, an isotropic

tangential friction with a friction coefficient μ_s = 0.3 was introduced between the CFRP plate and the steel substrate in the transverse direction. The CFRP and the steel substrate were modelled using 8-node linear brick elements of type C3D8R with reduced integration and hourglass control, while the hard plate and the clamp were modelled using 10-node quadratic tetrahedron elements of type C3D10. The elements had an overall dimension of approximately 2 mm.

In the first stage, a static uniform pressure of 396 MPa was introduced on the clamp plate over the contact area of the bolt head, which is a round area with outer and inner diameters of 20 and 13 mm, respectively (see Figure 4a) to simulate the prestressing force of 72 kN per bolt. This force level is generated in M12 high-strength bolts upon fastening them with an allowable torque of 160 N·m. In the next stage, a uniform displacement-controlled loading was applied to the free edge of the CFRP plate to evaluate the anchorage capacity of the joint before slippage of the CFRP. As mentioned earlier, the FE model was generated to check the stresses in the clamp plate and optimize its thickness. Afterwards, a parametric study was performed to optimize the fillet dimension of the hard plate to obtain an approximately uniform contact pressure between the hard plate and the CFRP reinforcement.

3.2.2. *FE results*

Figure 4b shows the von Mises' stresses in the FE model when the full bolts load is applied on the clamp plate, and the CFRP plate is pulled up to its tensile strength. It can be seen that by using 25 mm-thick clamp plates, manufactured from M200 steel with a nominal yield strength of σ_y = 1000 MPa, the maximum stress in the clamp plate is below $0.6\sigma_y$.

Figure 5a illustrates the effect of the hard plate fillet dimension (d) on the distribution of the contact pressure between the hard plate and the CFRP reinforcement. It can be seen from the figure that having no fillet results in a singular stress concentration on the CFRP edges, while there is no contact pressure in the middle width of the CFRP plate. The parametric study demonstrated that a fillet dimension of 10 mm with an inclination angle of 1.5° is the

optimal configuration for the hard plate to achieve a more uniform contact pressure on the CFRP plate. Note that round fillets with a radius of 2 mm were also considered in the longitudinal direction of the hard plates to avoid any undesired stress concentration.

Using the FE model of the optimized mechanical clamps (obtained through the abovementioned parametric study), the stress–elongation response of the CFRP plate was estimated and is provided in Figure 5b. FE results presented in Figure 5b suggest that the proposed mechanical clamp is capable of carrying the entire tensile capacity of the CFRP plate (nominal value of $\sigma_{f,u}$ = 2800 MPa) before any slippage of the clamp. It is obvious that the ultimate capacity of the proposed anchorage system is a function of the friction coefficient μ_s between the CFRP plate and the steel substrate. It has been demonstrated in [26] that $\mu_s \geq$ 0.3 can be expected by using diamond friction shims. Therefore, it may be concluded that by considering μ_s = 0.3, the ultimate capacity of the designed system, obtained from the FE modeling, is on the safe side.

4. Experimental Verification

4.1. Test Specimens

Two sets of tensile tests were carried out in this study. First, a set of tensile tests was performed on the so-called clamp test specimens, as depicted in Figure 6a, to evaluate the ultimate capacity and fatigue performance of the proposed mechanical clamping system for the fatigue strengthening of tensile steel members. Secondly, the performance of the proposed mechanical clamping system was compared to that of the conventional adhesively bonded solutions through a series of static tensile tests.

The second set of the experiments consisted of six static tensile tests on steel plates with overall dimensions of 1100 × 150 × 10 mm (length × width × thickness) as follows: one unstrengthened steel plate as the reference specimen depicted in Figure 6b; two steel plates strengthened with nonprestressed bonded CFRP reinforcement with normal modulus (NM)

and ultra-high modulus (UHM) of elasticity, hereafter called specimens *NPBR-NM* and *NPBR-UHM*, respectively (see dimensions in Figure 6c); one steel plate with the same configuration as that depicted in Figure 6c, strengthened with prestressed bonded NM CFRP reinforcements, hereafter called specimen *PBR-NM*; and two steel plate specimens as illustrated in Figure 6d strengthened with the proposed mechanical clamping system, one with nonprestressed NM CFRPs (hereafter called *NPUR-NM*) and the other one with prestressed NM CFRPs (hereafter called *PUR-NM*). It is worth mentioning that, because of the brittle nature and relatively low tensile strength of the UHM CFRP plates, it is almost impractical to clamp and/or prestress such composites [18,24]. Therefore, UHM CFRP plates were only used as a nonprestressed bonded solution (NPBR-UHM) and no other configuration (such as PBR-UHM, NPUR-UHM, and PUR-UHM) was included in the test layout.

Several electrical foil strain gauges were mounted on all the specimens to monitor the strain levels in the CFRP plates and steel substrate during the static and fatigue tests. Strain gauges of type 1-LY61-6/120 and 1-LY66-6/120 (HBM AG, Germany) with an electrical resistance of 120Ω ± 0.30% were mounted at mid-length of the steel and CFRP plates, respectively (see Figure 6 for the strain gauges' locations).

4.2. Material Properties

With the exception of the mechanical components of the proposed clamping system, which were made from high strength M200 steel, the utilized steel plates in all the experiments were of type S355J2+C with a nominal yield strength of 355 MPa. The Young's modulus of the steel (E_s) was determined as 200.9 GPa. Moreover, unidirectional UHM CFRP plates of type Carbolam THM 450-50×1.2 were used in specimen NPBR-UHM, while unidirectional NM CFRP plates of type S&P 150/2000 were used for the strengthening of the other steel plate specimens. The mechanical properties of the CFRP plates are provided in Table 1.

In the specimens strengthened using adhesively bonded CFRP reinforcements, a two-component epoxy adhesive, Araldite 420 A/B, was used. Sets of auxiliary tests were conducted on room-temperature cured samples to characterize the tensile properties and glass transition temperature (T_g) of the aforementioned adhesive. Table 2 summarizes the experimental results of these sets of auxiliary tests on the epoxy adhesive. Further details regarding these material characteristic tests can be found in [37]. Note that no auxiliary test was performed to determine the shear modulus of the adhesive as part of the present study; however, G_a = 730 MPa was used in the analytical model based on the manufacturer's catalogue for room-temperature applications.

4.3. CFRP Strengthening Procedure

4.3.1. *Nonprestressed reinforcement*

In order to strengthen the steel plate specimens using nonprestressed bonded CFRP plates, the bond area was first sand-blasted and carefully cleaned with acetone. CFRP plates were then glued on each side of the prepared steel surfaces using the two-component epoxy adhesive to realize the final configuration depicted in Figure 6c. The specimens were then cured at room temperature for six days before testing. On the other hand, strengthening of the steel plates using the mechanical unbonded clamps was much faster, as the clamps work based on friction, and neither surface preparation of the steel plate nor curing for the adhesive was required.

Different components of the proposed mechanical clamping system are illustrated in Figure 7a. In total eight high strength bolts were used in each of the clamp sets, and they were tightened with a torque of 160 N·m. Therefore, specimen NPUR-NM was easily prepared by putting different components of the mechanical clamping system together and tightening the M12 bolts of each clamp set, which tied the CFRP plates to the steel substrate. As previously mentioned, 3M^{TM} diamond friction shim was used between the CFRP and steel to increase the

CFRP-steel interface friction. Figure 7b illustrates an SEM image of the nickel-diamond coating on the 3M^{TM} friction shim.

4.3.2. *Prestressed reinforcement*

To strengthen the steel plate specimens with prestressed bonded and unbonded CFRP reinforcements (specimens PBR-NM and PUR-NM), a special prestressing setup was designed and assembled at the Structural Engineering Research Laboratory of Empa to simultaneously prestress two parallel CFRP plates (Figure 8). The distance between the two CFRPs was accurately kept at 10.40 mm using high strength steel cubes in the prestressing grips. CFRP plates were prestressed up to a total load level of 120 kN (approx. 30% of the tensile strength of the composite) using a hollow plunger hydraulic cylinder. The total prestressing load and the prestrain level in CFRP plates were monitored using a 300 kN load cell and the strain gauges mounted on the CFRPs, respectively.

Upon reaching the desired prestressing force in the CFRP plates of specimen PBR-NM, the epoxy adhesive was applied to the sand-blasted steel surfaces and the specimen was placed in between the CFRP plates. The prestressing force was kept constant for 6 days, and afterwards gradually released to zero. By contrast, as can be seen in Figure 9, the entire prestress and release process for specimen PUR-NM was completed in less than one hour owing to the fact that after prestressing, the CFRP plates were immediately anchored to the steel substrate using the newly developed mechanical clamping system. After tightening the prestressed bolts, the prestressing load was gradually decreased to zero. This resulted in a slight decrease in the prestrain level of the CFRP reinforcements owing to the compressive deformation of the steel substrate (see Figure 9). At this state, the average compressive strain on both sides of the steel plate was 368 μm/m, which corresponds to a compressive stress of 73.9 MPa. Next, the CFRP plates were cut from both extremities to realize the configuration depicted in Figure 6d. The prestressed specimens were then taken to the tensile testing machine.

4.4. Static and Fatigue Test Setup

A 1-MN static/fatigue servo-hydraulic Schenck machine with an Instron controller was used to perform the static and fatigue tensile tests. Figure 10a shows the test setup and the instrumentation used to monitor the specimens during static and fatigue testing. All the static tests were performed under displacement-controlled conditions at a speed of 1 mm/min, which was intentionally kept lower than the general recommendation provided in DIN EN ISO 6892-1 [38], in order to avoid any probable undesired strain dependency effects on the performance of the adhesively bonded reinforcements. The fatigue test on the mechanical clamping system (Figure 6a) was performed under load-controlled conditions with a load ratio ($R = T_{min}/T_{max}$) of 0.9, and a frequency of 15 Hz. The maximum load level (T_{max}) during the fatigue test was equal to 124 kN, which corresponded to 32% of the nominal tensile strength of the utilized CFRP. It should be noted here that a range of R = 0.1–0.3 is deemed representative of the practical fatigue load ratio range experienced by most of the fatigue-prone members in metallic bridges (see for example [28]). Assuming R = 0.2 for a tensile metallic member which needs to be strengthened, the load ratio experienced by the prestressed CFRP reinforcements (the developed PUR system) can be estimated approximately as R = 0.9 using the analytical model proposed in Section 2.1 (for the specific configuration given in Figure 6d). Consequently, to simulate the real stress state, experienced by the proposed mechanical clamping system, a relatively high load ratio (i.e., R = 0.9 in this case) was incorporated in the fatigue test.

5. Results and Discussion

5.1. Static and Fatigue Tests on the Proposed Mechanical Clamping System

Figure 10b illustrates the load–deformation response of the three clamp test specimens, monotonically loaded until failure. It can be seen in the figure that when double-sided sand paper was used between the CFRP plate and the steel substrate, the friction joint behaved relatively softer, while at 60% of the CFRP tensile strength, the stiffness of the joint dropped

to almost zero and the unstable slippage of the system occurred. On the other hand, when diamond friction shims were used to increase the interface friction of the CFRP-steel joint, no reduction in the joint stiffness or slippage of the clamps was observed until the tensile rupture of the CFRP plates occurred.

In order to investigate the fatigue performance of the proposed mechanical clamping system, the third clamp test specimen was first subjected to 10 million fatigue cycles with T_{max} = 124 kN and R = 0.9. Afterwards, a monotonic loading was applied on the specimen until the ultimate strength of the CFRP plates was reached. The experimental results provided in Figure 10b demonstrate that the proposed mechanical clamping system is capable of transferring the entire tensile capacity of the CFRP plates to the steel substrate, even after experiencing 10 million fatigue cycles.

The maximum bending strain generated in the mechanical clamps is plotted against the applied torque on the eight M12 (grade 12.9) bolts of the system in Figure 11a. It can be seen in the figure that the maximum bending strain, generated in the clamp plates at the allowable torque of 160 N·m, was approximately equal to 3000 μm/m which corresponded to a maximum bending stress of almost 600 MPa (considering E_s = 200 GPa). This stress level is equal to $0.6\sigma_y$, i.e., the allowable stress limit which was initially considered to design the clamp plate. Consequently, a comparison of the experimental values provided in Figure 11a with the FE results presented in Figure 4 reveals that a good correlation exists between the experimental and FE results in terms of the maximum bending stress in the clamp plates (see Section 3.2.2).

The maximum strain levels in the clamp plates were monitored during the 10 million fatigue cycles, and their evolution with respect to the elapsed fatigue cycles are provided in Figure 11b. The figure reveals that the maximum bending strain in the clamp plates was slightly reduced by approximately 1.5% over 10 million fatigue cycles, which indirectly indicates that the prestressing force in the M12 bolts was reduced by almost 1.5%. This is

believed to be due to the creep of the composite matrix in the transverse direction, while this level of prestress loss in the bolts over 10 million fatigue cycles is deemed acceptable for the proposed mechanical clamping system.

5.2. Static Tests on CFRP-Strengthened Steel Plates

Load–strain responses of all the specimens, tested under uniaxial monotonic loading in the second sets of the experiments are plotted in Figure 12, while the results are summarized in Table 3. As stated earlier, *fatigue* strengthening of metallic members is the main focus of the current study. Therefore, all the specimens were subjected to uniaxial tensile loads equal to 300 kN, which corresponded to approximately $0.5\sigma_y$ in the bare (unstrengthened) steel, and therefore can fairly represent the high-cycle fatigue problem in such steel members [15].

Figure 12 illustrates that strengthening of the steel plate specimens using nonprestressed bonded or unbonded CFRP reinforcements slightly increased the stiffness of the member within the strengthened length, while this stiffness improvement is almost identical for the case of bonded and unbonded solutions. As expected, utilizing nonprestressed bonded UHM CFRP reinforcements further improved the stiffness of the steel member as the strain in the mid-length of the steel plate at T = 300 kN was reduced by 16.3% compared to the reference unstrengthened specimen.

Figure 12 obviously shows the great advantage of using prestressed CFRP reinforcements to reduce the tensile strain level in the steel substrate under external loading. However, the two prestressed bonded CFRP plates in specimen PBR-NM were debonded from the steel substrate at relatively very low levels of the external tensile load, T = 50 and 153 kN, respectively. As can be seen in Figure 12, the brittle debonding failure started at the extremity of the prestressed CFRP reinforcements and rapidly propagated towards the mid-length of the specimen. Debonding in this case is generally attributed to the fact that prestress force release generated considerable interfacial shear stresses in the CFRP end zones [20,21]. The external tensile loading on the CFRP-steel joint then increased the accumulated

interfacial shear stresses, which resulted in the debonding failure of the prestressed CFRP reinforcement at the critical external load level. This experimental observation is in accordance with the interpretation provided at the end of Section 2.2. By contrast, the developed mechanical clamping system, used to strengthen specimen PUR-NM, could carry the prestressing force up to the end of loading procedure; the system experienced no slippage (see Figure 12).

Load–strain behavior of the strengthened specimens was predicted by the proposed analytical models (presented in Section 2), and the predictions are also plotted in Figure 12 for comparison purposes. As the load–strain responses of the tested specimens (illustrated in Figure 12) were directly obtained from the experiments, the analytical formulations of the stress in the steel substrate, presented in Section 2 (i.e., Eq. (1) for the case of unbonded, and Eq. (15) for the case of bonded reinforcements), were translated into strain functions using Hooke's law. Note that in Eqs.(1) and (15), $y = 0$ was incorporated, owing to the fact that the strain gauges were installed at mid-length of the steel specimens (see Figure 6) as the state of stresses at this location of the strengthened plates was the most interesting.

It can be concluded from Figure 12 that the proposed analytical models are capable of accurately predicting the behavior of non-prestressed and prestressed CFRP-strengthened steel plates, both in the case of bonded and unbonded solutions. As mentioned earlier, linear-elastic behavior of all the individual elements of the joint (i.e. steel, CFRP, and adhesive) is the main assumption of the developed analytical models. This assumption, however, applies when fatigue strengthening of existing metallic members is of interest.

Figure 13 shows the efficiency of the different strengthening solutions utilized in this study in terms of strain reduction in the steel substrate compared to the reference unstrengthened specimen at $T = 300$ kN. It can be concluded from the figure that the efficacy of having relatively high prestressing forces in the NM CFRP reinforcements is much higher than the stiffness improvement obtained by using UHM CFRPs. This is important when

fatigue crack prevention or fatigue crack arrest is of interest in metallic members, given that in practical strengthening projects the application of UHM CFRP materials may be much more expensive than using the proposed PUR system.

6. Conclusions and Recommendations

Based on the analytical modeling and experimental test results, provided in the current study, the following conclusions can be drawn:

- Sets of static and fatigue tests, performed on the proposed mechanical clamping system, revealed that the proposed unbonded friction-based system is capable of transferring the entire tensile capacity of the CFRP plates to the steel substrate, even after experiencing 10 million fatigue cycles. Further experimental tests on the steel plate specimens strengthened with the proposed PUR system confirmed the high performance of the system, as no slippage/failure was observed.
- Uniaxial tensile tests were performed on the reference unstrengthened and CFRP-strengthened steel plates up to approximately $0.5\sigma_y$ in the bare steel, which indeed represents the maximum stress level experienced by structural metallic members in high-cycle fatigue regime. Experimental results demonstrated that the use of nonprestressed bonded/unbonded CFRP reinforcements can slightly enhance the stiffness of the member within the strengthened length; this stiffness improvement is almost identical for the case of bonded and unbonded solutions.
- Static test results on CFRP-strengthened steel plates revealed that the efficacy of having relatively high prestressing forces in the NM CFRP reinforcements is much higher than the stiffness enhancement obtained by using UHM CFRPs. This conclusion can be certainly important when fatigue strengthening of existing metallic members is of interest, owing to the fact that in practical strengthening projects application of UHM CFRP materials can be much more expensive than using the proposed PUR system.

Although application of prestressed UHM CFRP plates could be an idealized solution for fatigue strengthening of metallic members, the brittle nature of the UHM CFRP composites makes their practical prestressing solutions almost impossible.

- Experimental results of the current study showed that even though adhesively bonded CFRPs can transfer certain levels of prestressing force to the steel substrate, the available bond capacity of the PBRs is relatively low for carrying the external loads on the strengthened member. More research would be needed to further investigate the bond behavior and debonding capacity of PBR solutions, in particular to better realize the coupled effects of moderately high service temperatures, creep, and fatigue.
- A very good correlation was observed between the experimental test results of the CFRP-strengthened steel plates and the predictions of the proposed simple analytical models. The models can be used to estimate the stress levels in the CFRP-strengthened tensile steel members subjected to temperature change and external loading in the elastic regime for both adhesively bonded and mechanically clamped CFRP plates. The analytical models also take into account the prestrain level in the CFRP reinforcements.
- Owing to the advantages of the proposed PUR system including its fast application, elimination of any surface preparation and adhesive curing procedure, high performance of the system in terms of prestressing levels, and insensitivity of the proposed system to high service temperatures, the PUR system can be used as a better alternative to the conventional adhesively bonded solutions for static and/or fatigue strengthening of existing tensile metallic members.
- The mechanical clamping system, developed in this study, was designed to clamp a pair of prestressed CFRP plates (i.e., one reinforcement plate on each side of the steel substrate). Nevertheless, in practical applications, the prestressing force that is provided by a pair of CFRP plates might not be sufficient to prevent fatigue crack initiation or to arrest the propagation of an existing fatigue crack. In such cases, several sets of the

proposed PUR system can be used in parallel, if possible. Alternatively, similar mechanical clamping systems, capable of holding multiple prestressed CFRP plates, need to be developed. It is believed that the knowledge and the understanding which has been gained through this work would certainly help to design such mechanical clamping systems. It is also worth noting that the abovementioned concluding remarks are based on limited sets of experimental tests, while a more comprehensive test layout with statistically sufficient test repetition has to be performed in future research studies in order to provide a reliable probabilistic basis and determine proper partial safety factor values.

Acknowledgements

This paper is an extended version of the authors' paper presented in SMAR 2017 conference, 13–15 September 2017, ETH Zurich, Switzerland. The authors gratefully acknowledge the financial support provided by the Swiss National Science Foundation (SNSF Project No. 200021–153609) and the Australian Research Council (ARC) Linkage Grant (LP140100543). The authors would like to thank the technicians of the Structural Engineering Research Laboratory, Mechanical Systems Engineering Laboratory, and the Central Workshop of Empa for their exceptional cooperation in manufacturing the mechanical parts and performing the experiments. Special thanks also go to Robin Pauer at the Electron Microscopy Center of Empa for his kind assistance with scanning electron microscopy. Finally, the support of S&P Clever Reinforcement Company AG, Switzerland, who provided the materials for the current study, is acknowledged.

References

1. Zhao XL. FRP-strengthened metallic structures. CRC Press, 2013.

2. Zhao XL, Zhang L. State-of-the-art review on FRP strengthened steel structures. Engineering Structures. 2007;29(8):1808-23.

3. El-Tahan M., Dawood M., Song G. Development of a self-stressing NiTiNb shape memory alloy (SMA)/fiber reinforced polymer (FRP) patch. Smart Materials and Structures. 2015;24(6):065035.

4. Rizkalla S., Dawood M., Schnerch D. Development of a carbon fiber reinforced polymer system for strengthening steel structures. Composites - Part A. 2008;39(2):388-97.

5. Schnerch D., Dawood M., Rizkalla S., Sumner E. Proposed design guidelines for strengthening of steel bridges with FRP materials. Construction and Building Materials. 2007;21(5):1001-10.

6. Deng J., Lee M.M.K. Behaviour under static loading of metallic beams reinforced with a bonded CFRP plate. Composite Structures. 2007;78(2):232-42.

7. Deng J., Lee M.M.K., Moy S.S.J. Stress analysis of steel beams reinforced with a bonded CFRP plate. Composite Structures. 2004;65(2):205-15.

8. Colombi P., Fava G. Fatigue crack growth in steel beams strengthened by CFRP strips. Theoretical and Applied Fracture Mechanics. 2016;85:173-82.

9. Colombi P., Fava G., Poggi C., Sonzogni L. Fatigue reinforcement of steel elements by CFRP materials: Experimental evidence, analytical model and numerical simulation. Procedia Engineering. 2014;74:384-7.

10. Colombi P., Fava G., Sonzogni L. Fatigue crack growth in CFRP-strengthened steel plates. Composites Part B: Engineering. 2015;72:87-96.

11. Deng J., Lee M.M.K. Fatigue performance of metallic beam strengthened with a bonded CFRP plate. Composite Structures. 2007;78(2):222-31.

12. Mustafa S.A.A., Moy S.S.J. Strengthening cast iron struts using carbon fibre reinforced polymers - Finite element modelling. Composites Part B: Engineering. 2011;42(5):1048-56.

13. Ghafoori E, Schumacher A, Motavalli M. Fatigue behavior of notched steel beams reinforced with bonded CFRP plates: Determination of prestressing level for crack arrest. Engineering Structures. 2012;45:270-83.

14. Ghafoori E, Motavalli M, Botsis J, Herwig A, Galli M. Fatigue strengthening of damaged metallic beams using prestressed unbonded and bonded CFRP plates. International Journal of Fatigue. 2012;44:303-15.

15. Hosseini A, Ghafoori E, Motavalli M, Nussbaumer A, Zhao X-L. Mode I fatigue crack arrest in tensile steel members using prestressed CFRP plates. Composite Structures. 2017;178:119-34.

16. Ghafoori E, Motavalli M, Nussbaumer A, Herwig A, Prinz G, Fontana M. Determination of minimum CFRP pre-stress levels for fatigue crack prevention in retrofitted metallic beams. Engineering Structures. 2015;84:29–41.

17. Ghafoori E, Motavalli M, Nussbaumer A, Herwig A, Prinz GS, Fontana M. Design criterion for fatigue strengthening of riveted beams in a 120-year-old railway metallic bridge using pre-stressed CFRP plates. Composites Part B: Engineering. 2015;68:1-13.

18. Ghafoori E, Motavalli M, Zhao XL, Nussbaumer A, Fontana M. Fatigue design criteria for strengthening metallic beams with bonded CFRP plates. Engineering Structures. 2015;101:542-57.

19. Koller RE, Stoecklin I, Weisse B, Terrasi GP. Strengthening of fatigue critical welds of a steel box girder. Engineering Failure Analysis. 2012;25:329-45.

20. Hosseini A, Ghafoori E, Wellauer M, Sadeghi Marzaleh A, Motavalli M. Short-term bond behavior and debonding capacity of prestressed CFRP composites to steel substrate. Engineering Structures. 2018;176:935-947.

21. Martinelli E, Hosseini A, Ghafoori E, Motavalli M. Behavior of prestressed CFRP plates bonded to steel substrate: numerical modeling and experimental validation. Composite Structures. 2018;207:974-984.

22. Nakamura H, Yamamura Y, Ito H, Lin F, Maeda K. Development of Pre-Tensioning Device for CFRP Strips and Applicability to Repair of Cracked Steel Members. Advances in Structural Engineering. 2014;17(12):1705-17.

23. Emdad R, Al-Mahaidi R. Effect of prestressed CFRP patches on crack growth of centre-notched steel plates. Composite Structures. 2015;123:109-22.

24. Ghafoori E, Motavalli M. Normal, high and ultra-high modulus CFRP laminates for bonded and un-bonded strengthening of steel beams. Materials and Design. 2015;67:232–43.

25. Ghafoori E, Motavalli M. Lateral-torsional buckling of steel I-beams retrofitted by bonded and un-bonded CFRP laminates with different pre-stress levels: experimental and numerical study. Construction and Building Materials. 2015;76:194–206.

26. Ghafoori E, Motavalli M. Innovative CFRP-Prestressing System for Strengthening Metallic Structures. Journal of Composites for Construction. 2015;19(6):04015006.

27. Kianmofrad F, Ghafoori E, Elyasi MM, Motavalli M, Rahimian M. Strengthening of metallic beams with different types of pre-stressed un-bonded retrofit systems. Composite Structures. 2017;159:81-95.

28. Hosseini A, Ghafoori E, Motavalli M, Nussbaumer A, Zhao XL, Al-Mahaidi R. Flat prestressed unbonded retrofit system for strengthening of existing metallic I-Girders. Composites Part B: Engineering. 2018;155:156-72.

29. Ghafoori E, Hosseini A, Al-Mahaidi R, Zhao XL, Motavalli M. Prestressed CFRP-strengthening and long-term wireless monitoring of an old roadway metallic bridge. Engineering Structures. 2018;176:585-605.

30. Hosseini A, Ghafoori E, Motavalli M, Nussbaumer A, Al-Mahaidi R, Terrasi G. A novel mechanical clamp for strengthening of steel members using prestressed CFRP plates. In: Proceedings of the Fourth Conference on Smart Monitoring, Assessment and Rehabilitation of Civil Structures (SMAR 2017), Zurich, 13-15 September, 2017.

31. Hart-Smith LJ. Adhesive-bonded double-lap joints. NASA-CR-112235, 1973.

32. Albat A, Romilly D. A direct linear-elastic analysis of double symmetric bonded joints and reinforcements. Composites Science and Technology. 1999;59(7):1127-37.

33. Hosseini A, Ghafoori E, Motavalli M, Nussbaumer A, Zhao X-L. Stress Analysis of Unbonded and Bonded prestressed CFRP-Strengthened Steel Plates. In: Proceedings of 8th International Conference on Fiber Reinforced Polymer (FRP) Composites in Civil Engineering (CICE2016). Hong Kong, 14-16 December 2016, p. 1179-86.

34. Täljsten B, Hansen CS, Schmidt JW. Strengthening of old metallic structures in fatigue with prestressed and non-prestressed CFRP laminates. Construction and Building Materials. 2009;23(4):1665-77.

35. Volkersen O. Die Nietkraftverteilung in zugbeanspruchten Nietverbindungen mit konstanten Laschenquerschnitten. Luftfahrtforschung. 1938;15:41-7.

36. ABAQUS U. Version 6.14-1. Providence, RI: Dassault Systémes Simulia Corp.; 2014.

37. Hosseini A, Barbezat M, Michels J, Ghafoori E, Motavalli M, Terrasi G. Glass transition evaluation of commercially available epoxy adhesives for strengthening of steel structures with bonded CFRP plates. In: Proceedings of 9th International Conference on Fibre-Reinforced Polymer (FRP) Composites in Civil Engineering (CICE2018). Paris, France, 17-19 July 2018.

38. ISO E. 6892-1. Metallic materials-Tensile testing-Part 1: Method of test at room temperature. International Organization for Standardization; 2009.

Table 1. Mechanical properties of CFRP plates in the fibers' direction.

Material	Type	Nominal tensile strength (MPa)	Elastic modulus (GPa)
NM CFRP	S&P 150/2000-50/1.4	2800	156 [33]
UHM CFRP	THM 450-50 × 1.2	1200	435 [24]

NM = normal modulus; UHM = ultra-high modulus

Table 2. Nominal average tensile strength, $\sigma_{a,u}$, strain at rupture, $\varepsilon_{a,u}$, elastic modulus, E_a, and glass transition temperatures for the utilized epoxy adhesive.

Type of test	Number of tested samples	Age of sample (d)	$\sigma_{a,u}$ (MPa)	$\varepsilon_{a,u}$ (%)	E_a (GPa)	T_o (°C)	T_i (°C)
Uniaxial tensile	6	7	24.6	9.28	1.68	-	-
DMTA	3	28	-	-	-	41.4	46.8

DMTA = dynamic mechanical thermal analysis

T_o = glass transition temperature corresponding to the onset point of the stiffness decrease of the dynamic modulus, E'

T_i = glass transition temperature corresponding to the inflation point of the E'–T diagram

Table 3. Static test specimens' description and test results.

Test No.	Specimen label	Total prestressing force (kN)	Maximum strain in steel at T = 300 kN (μm/m)	Strain reduction in steel compare with reference specimen at T = 300 kN (%)
1	Reference	-	995	-
2	NPBR-NM	-	931	6.4
3	NPUR-NM	-	925	7.0
4	NPBR-UHM	-	833	16.3
5	PBR-NM	120	Debonding failure	N.A.
6	PUR-NM	120	547	45.0

NPBR = nonprestressed bonded reinforcement; PUR = prestressed unbonded reinforcement

NPUR = nonprestressed unbonded reinforcement; NM = normal modulus

PBR = prestressed bonded reinforcement; UHM = ultra-high modulus

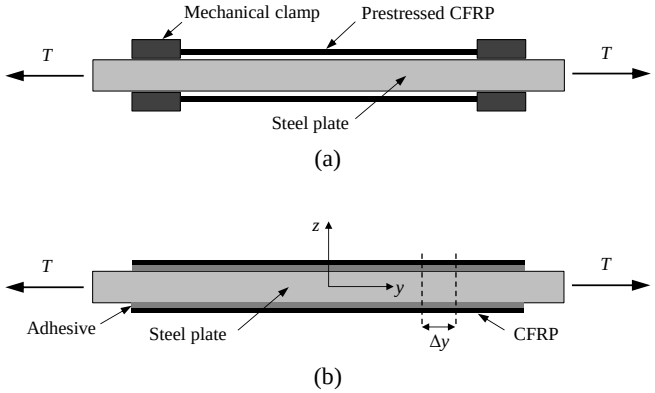

Figure 1. Schematic view of: (a) prestressed unbonded reinforcement (PUR) and (b) prestressed bonded reinforcement (PBR).

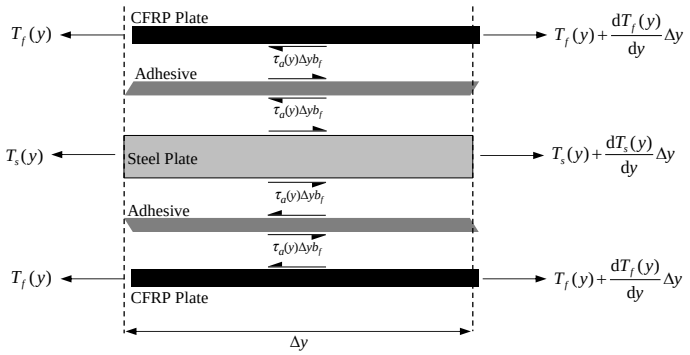

Figure 2. Free body diagram and force equilibrium in a finite element of a prestressed bonded CFRP-strengthened steel plate.

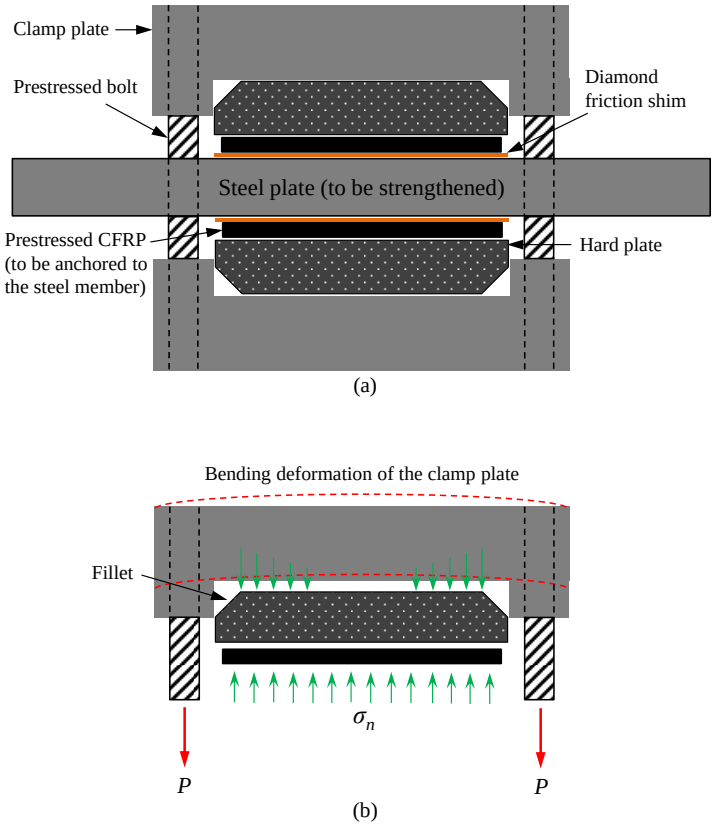

Figure 3. Schematic of proposed mechanical clamping system: (a) cross-sectional view; (b) stress transfer between different components.

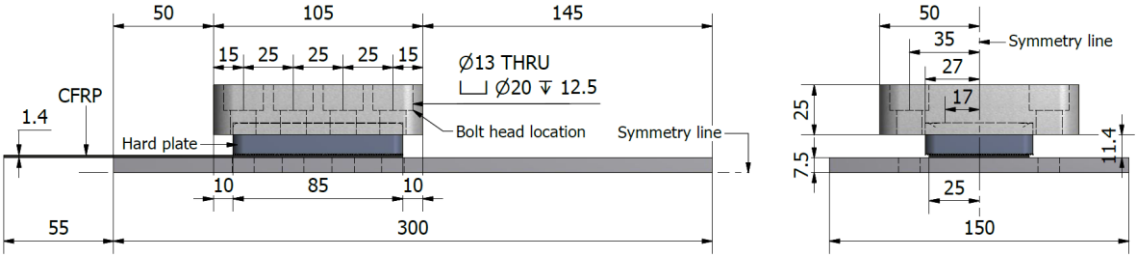

(a)

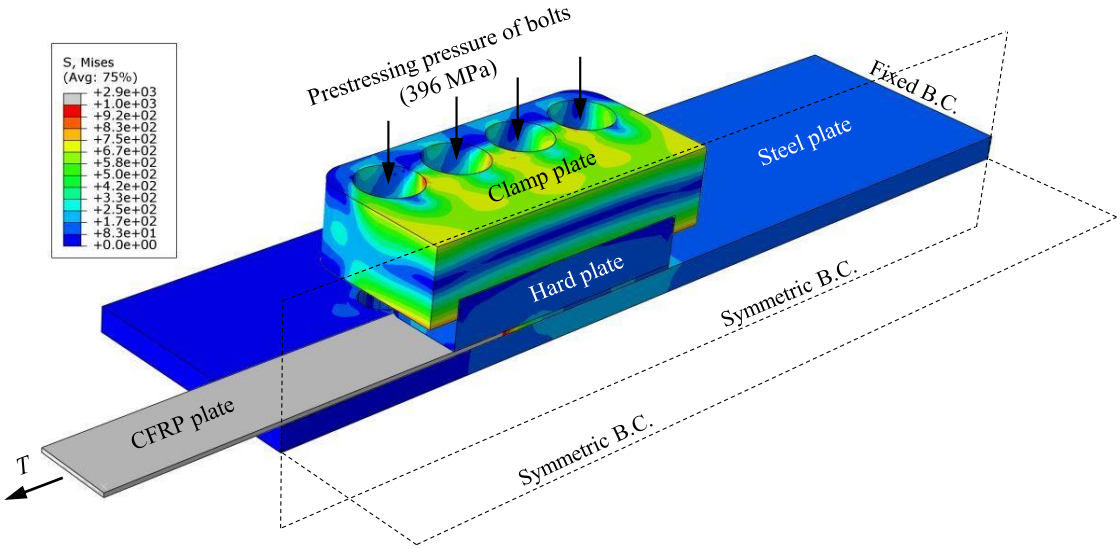

(b)

Figure 4. (a) Optimized dimensions used in the finite element simulation (all dimensions are in mm); (b) von Mises' stresses in the proposed mechanical clamping system when subjected to the allowable bolts load and CFRP tensile strength.

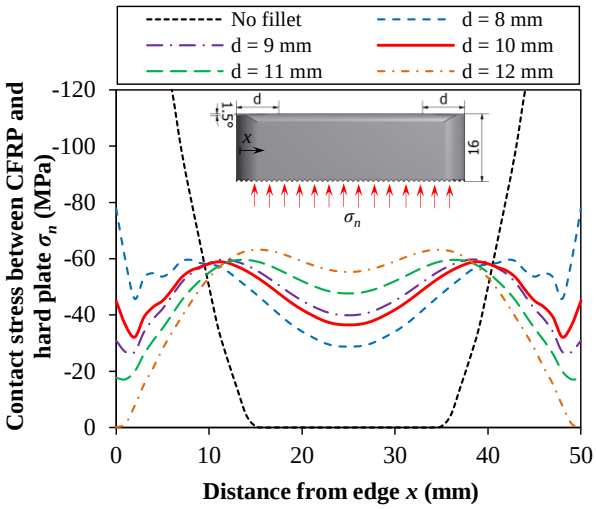

(a)

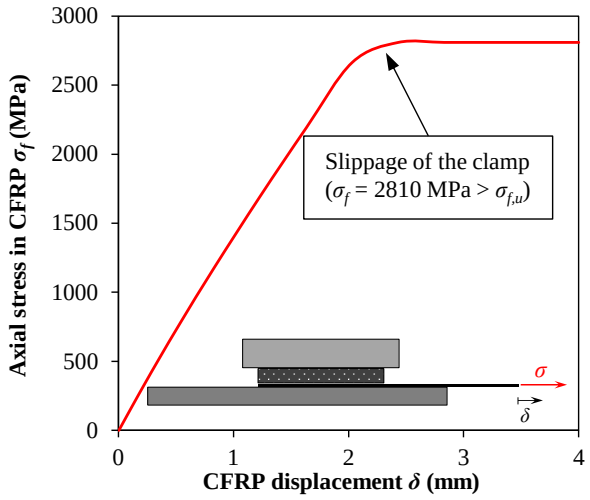

(b)

Figure 5. FE results: (a) effect of fillet dimension on distribution of contact pressure (d = fillet dimension); (b) ultimate capacity of joint before slippage of mechanical clamp.

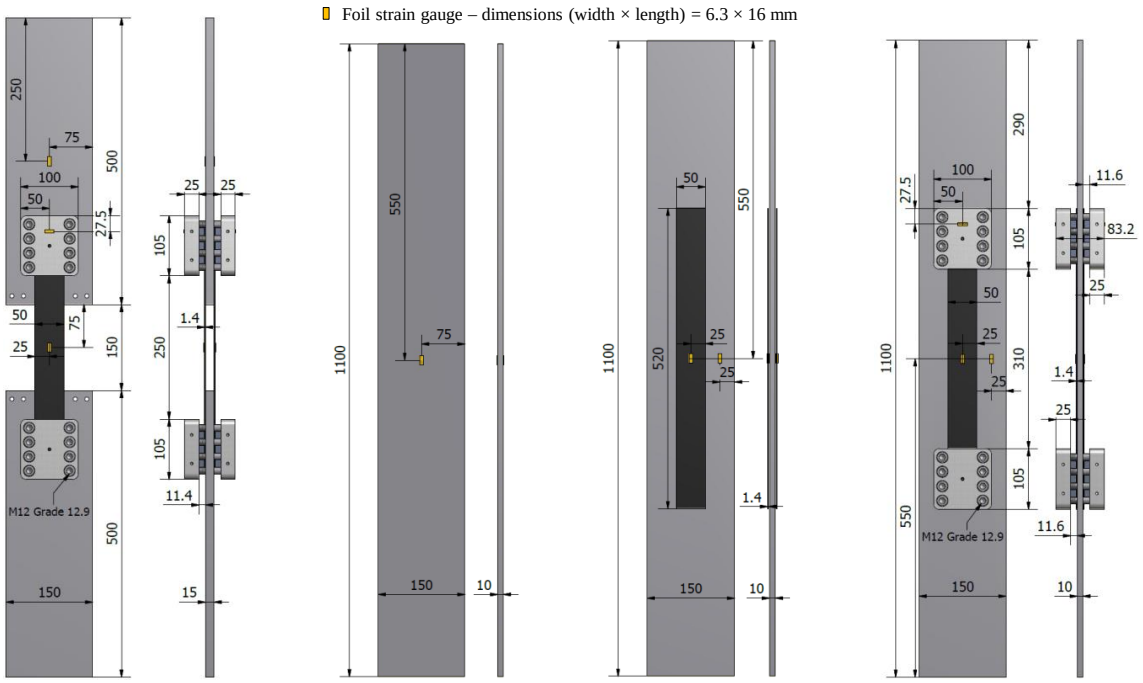

Figure 6. Dimensions of different test specimens and locations of the mounted strain gauges (all dimensions are in mm): (a) clamp test; (b) reference; (c) NPBR-NM, NPBR-UHM, and PBR-NM; (d) NPUR-NM, and PUR-NM.

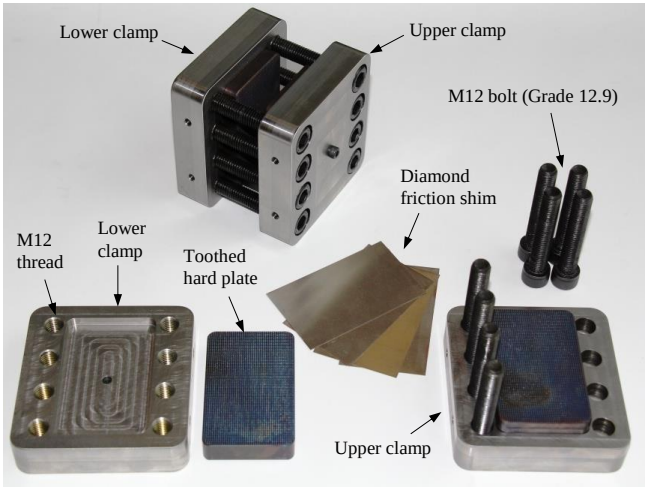

(a)

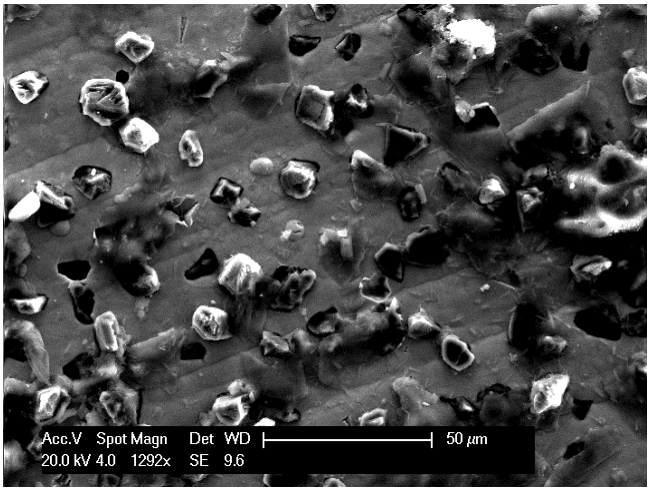

(b)

Figure 7. (a) Different components of proposed mechanical clamping system; (b) SEM image of nickel-diamond coating on 3M^{TM} friction shim (SEM performed at Empa).

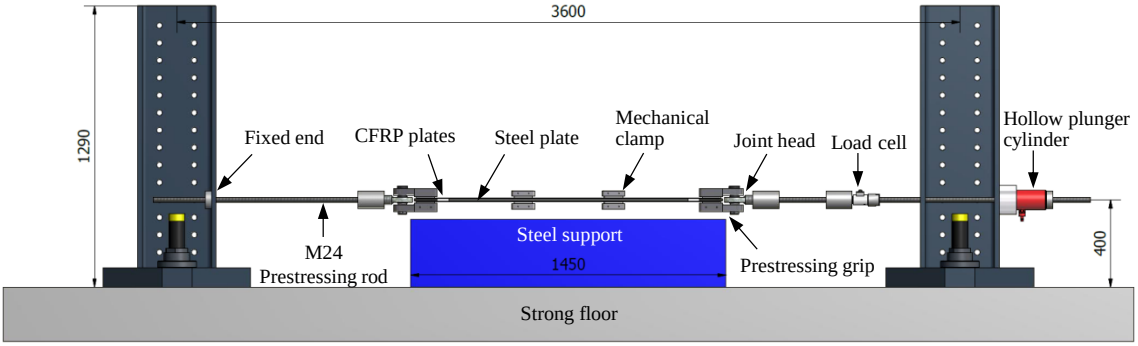

Figure 8. Prestressing setup.

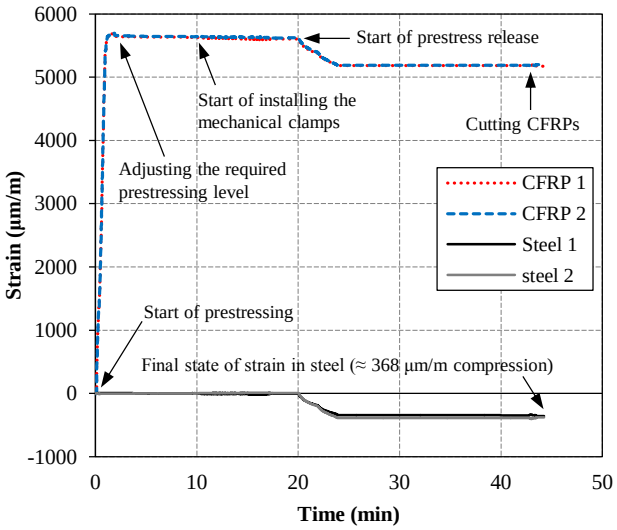

Figure 9. Strain history of steel and CFRP plates in PUR-NM specimen during prestress and release process.

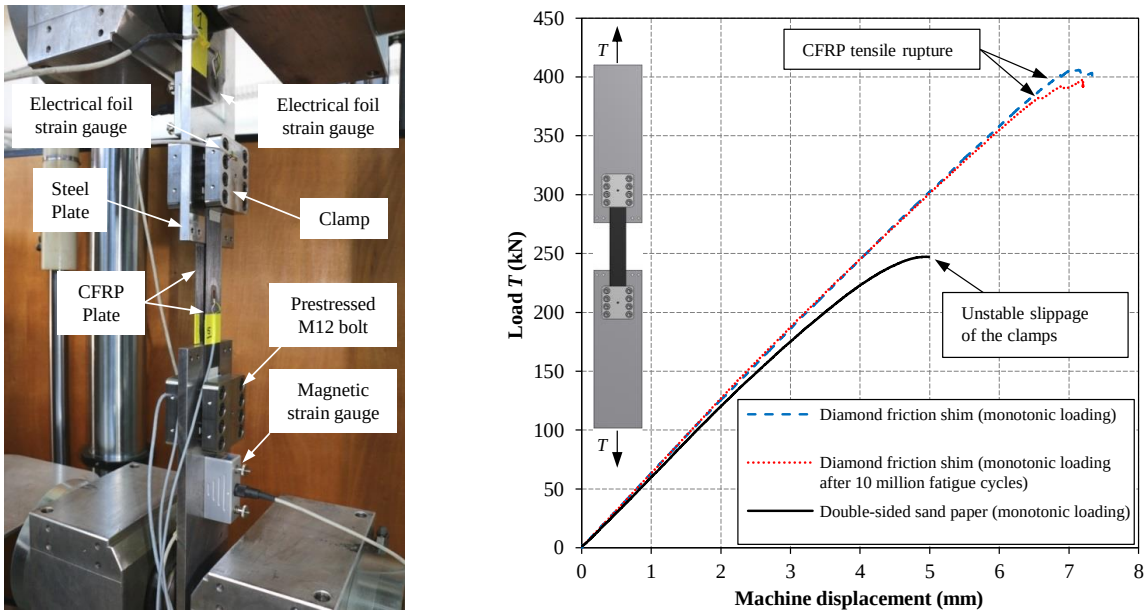

(a) (b)

Figure 10. (a) Test setup for static and fatigue experiments; (b) load–displacement response of clamp test specimens.

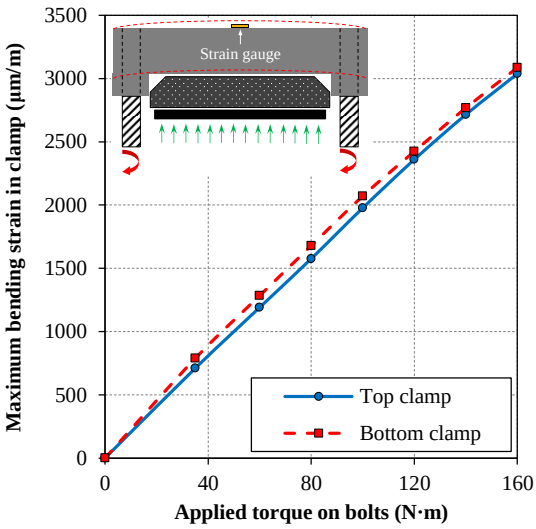

(a)

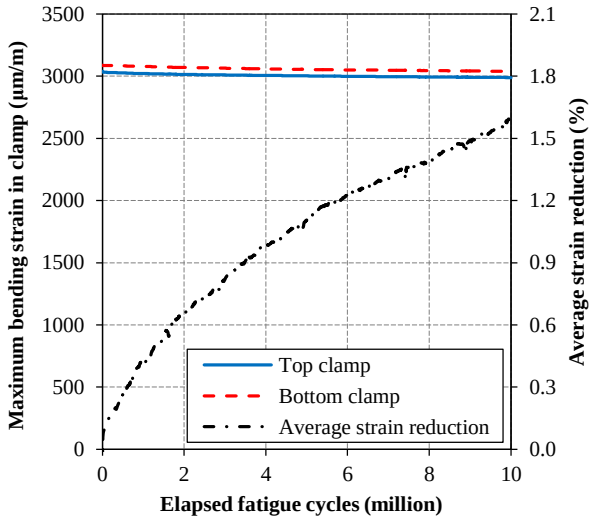

(b)

Figure 11. (a) Maximum bending strain in clamp plates versus applied torque; (b) evolution of maximum bending strain in mechanical clamps with respect to fatigue cycles.

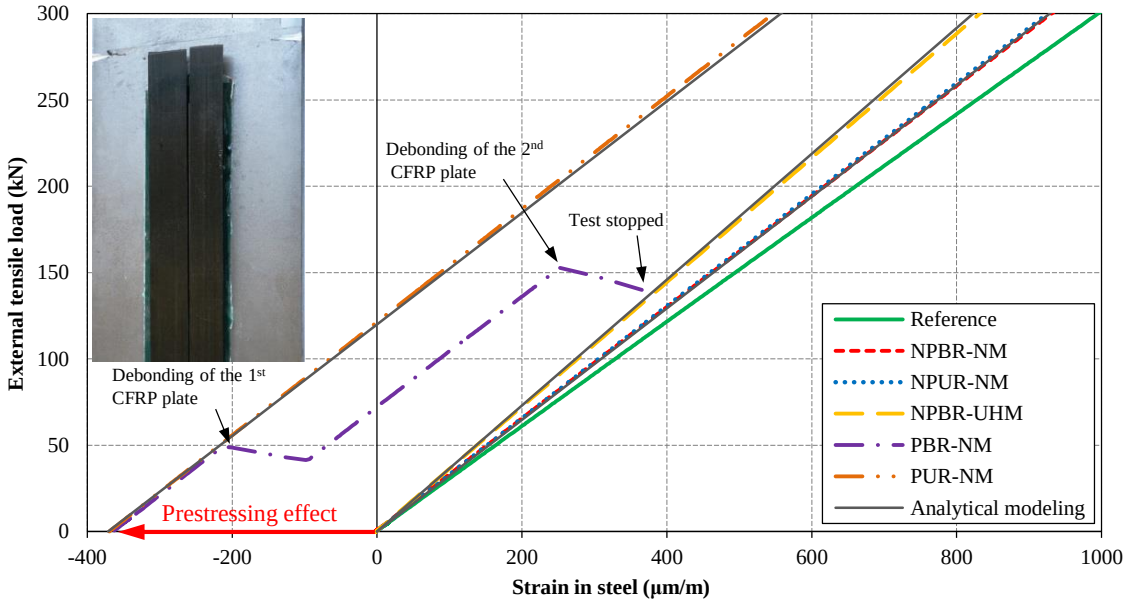

Figure 12. Load–strain response of tested specimens and model predictions.

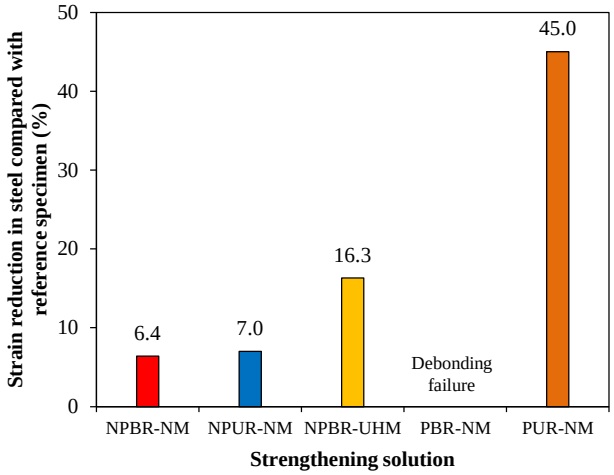

Figure 13. Efficiency of different strengthening solutions in terms of strain reduction in steel compared with reference specimen at T = 300 kN.